Cancer Imaging (2010) **10,** S172–S178
DOI: 10.1102/1470-7330.2010.9029

CI

e-med
www.e-med.org.uk

Whole-body diffusion-weighted imaging in lymphoma

C. Lin[a,b], E. Itti[c], A. Luciani[a], C. Haioun[d], M. Meignan[c] and A. Rahmouni[a]

Departments of [a]Radiology, [c]Nuclear Medicine and [d]Haematology, Centre Hospitalo-Universitaire Henri Mondor, 51, Avenue du Maréchal de Lattre de Tassigny, 94010 Créteil, France; [b]Department of Nuclear Medicine and Molecular Imaging Center, Chang Gung Memorial Hospital and University, 5 Fuxing Street, Gueishan 33305, Taoyuan, Taiwan

Corresponding address: Alain Rahmouni, Imagerie Medicale, Hopital Henri Mondor, 51 Av Marechal de Lattre de Tassigny, 94010 Créteil Cedex, France.
Email: alain.rahmouni@hmn.ap-hop-paris.fr

Abstract

The current evidence regarding the usefulness of whole-body diffusion-weighted magnetic resonance imaging (DWI) in lymphoma is reviewed. DWI is capable of combining anatomical and functional information and is becoming a valuable tool in oncology, in particular for staging purposes. DWI may prove to be a useful biomarker in clinical decision making for patients with lymphoma. Large-scaled prospective studies are needed to confirm these preliminary results.

Keywords: *Whole-body DWI; lymphoma; staging; response assessment; FDG-PET/CT.*

Introduction

Initially accepted as a diagnostic tool for patients with acute stroke, more applications of extracranial diffusion-weighted magnetic resonance imaging (DWI) are starting to emerge[1]. DWI probes random microscopic motion of water molecules in the body noninvasively[2]. Tumors are frequently more cellular than the tissue from which they originate and thus appear to be of relatively high signal intensity (restriction of water diffusion) on DWI providing qualitative analysis[3]. Microscopic motion of water molecules can also be quantitatively assessed by measuring the apparent diffusion coefficient (ADC) using at least two diffusion weighting measurements determined by the *b* values. In recent years, DWI has been extensively studied in oncology for differentiating between benign and malignant cervical lymph nodes or nodal staging[4–6], tumor detection and staging[7,8], tumor characterization[9], monitoring treatment response[10] and predicting treatment response and local recurrence rate after therapy[11–13].

Lymphoma lesions are usually well visualized on DWI because of their high cellularity and high nuclear-to-cytoplasm ratio. Lymphomas have been shown to have significantly lower ADC values compared with other tumor types in different body regions[8,14–16]. In lymphomas, therapeutic strategies, the patient's prognoses and treatment response monitoring all depend on accurate initial staging. Therefore, the development of whole-body DWI for lymphoma in which extensive nodal and extranodal involvement is common would be of great clinical importance.

Whole-body DWI protocol

Performing whole-body DWI is challenging mainly because of the inhomogeneity of the magnetic field over a large imaging area and motion arising from different organs that might degrade the image quality. The developments of echo-planar imaging (EPI), high-gradient amplitudes, multichannel coils, and parallel imaging play a major role in extending the applications of DWI. In particular, the introduction of parallel imaging, which enables reduction in the echo time (TE), echo-train length, and k-space filling time, led to substantially less motion artifacts during image acquisition, thus enabling high-quality diffusion-weighted images of the body to be obtained[3].

1470-7330/10/000001 + 7

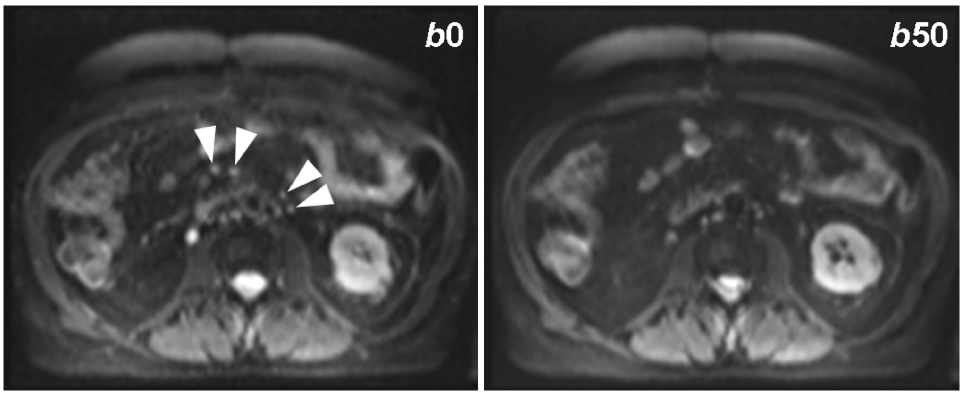

Figure 1 **Diffusion-weighted images with *b* values of 0 and 50 s/mm^2 (*b*0 and *b*50) in a 53-year-old patient with mediastinal diffuse large B-cell lymphoma. Tiny hyperintense dots (cross-sections of small vessels) on the *b*0 diffusion-weighted image (arrowheads) disappeared on the *b*50 diffusion-weighted image, which facilitates the detection of adjacent lymph nodes.**

In 2004, Takahara *et al.*[17] reported a unique concept of whole-body DWI using the short tau inversion recovery (STIR)-EPI sequence and free breathing scanning (diffusion-weighted whole-body imaging with background body signal suppression: DWIBS). STIR theoretically gives more homogeneous fat saturation because of its insensitivity to magnetic field heterogeneity and is commonly used[18]. Longer scanning time under free breathing allows multiple signal averaging in order to maintain good contrast-to-noise ratio[19] and thinner axial images (usually 4 mm in slice thickness with or without 1 mm overlap, but can be up to 6 mm) can be obtained for volumetric three-dimensional image processing[18]. Most studies used the body coil for signal reception[17,20–22]. Most recently, Kwee *et al*. used a 4-element phased-array surface coil (higher signal-to-noise ratio (SNR) than a body coil and allowing parallel imaging) that can move sequentially to image the separate stations of the whole-body DWI, without patient repositioning[23–25]. Total acquisition time covering from head to upper thighs ranged from 20 to 30 min depending on the parameters chosen[18,22,23]. Whole-body DWI is mostly evaluated qualitatively for lesion detection on inverted gray images acquired with a single *b* value in the range of 800–1000 s/mm^2 with fat suppression, resulting in positron emission tomography (PET)-like images[17,18]. Because anatomical details are lacking in these images, standard T1- and T2-weighted sequences remain indispensable to act as anatomical reference for the DWIBS images, in order to exactly localize lesions[18], therefore adding another acquisition time to the entire magnetic resonance (MR) examination.

Whole-body DWI can also be performed with a combined surface coil, allowing parallel imaging over the entire body, and improved spatial resolution. We designed a whole-body DWI 1.5 T MR (Siemens, Erlangen) protocol using exclusively a single-shot spin-echo EPI sequence with acquisition parameters detailed in Ref.[26]. Patients were positioned with five sets of integrated phased-array surface coils installed simultaneously (total imaging matrix system) to cover from head to upper thighs for signal reception. In order to more reliably assess ADC values on a whole-body scale, three trace *b* values, 50, 400 and 800 s/mm^2 (*b*50, *b*400 and *b*800) instead of the commonly used two data points, were used. Although ADC measurement of a large, relatively uniform organ such as the liver appears to be accurate with free breathing, respiratory motion can still result in ADC errors for small focal lesions such as lymph nodes because of signal contamination by adjacent tissues[19]. We therefore chose to perform whole-body image acquisition with respiratory gating in order to minimize slice position mismatch between different *b* values and different excitations[26]. Total acquisition time is longer in this case compared with that with free breathing. However, anatomical information can be obtained from *b*50 diffusion-weighted images therefore saving time for acquisition of standard T1- or T2-weighted images. Moreover, signals from vessels are eliminated on *b*50 diffusion-weighted images therefore allowing more selective visualization of adjacent lymph nodes (Fig. 1). Most perfusion effects can be reduced in this case compared with ADC calculation with the lowest *b* value set at 0. Spectrally selective fat saturation was used to achieve a reasonable total acquisition time (30–45 min) and a higher SNR than STIR (acquisition time twice as long)[26]. The centre of each stack of images (i.e. each station) was placed in the isocentre during acquisition with B0 shim for each station. To our knowledge, this is the only whole-body DWI protocol with respiratory gating proven feasible in a routine clinical setting. Image analysis was performed on source axial diffusion-weighted images with three *b* values as well as their corresponding ADC maps, including both qualitative and quantitative analyses.

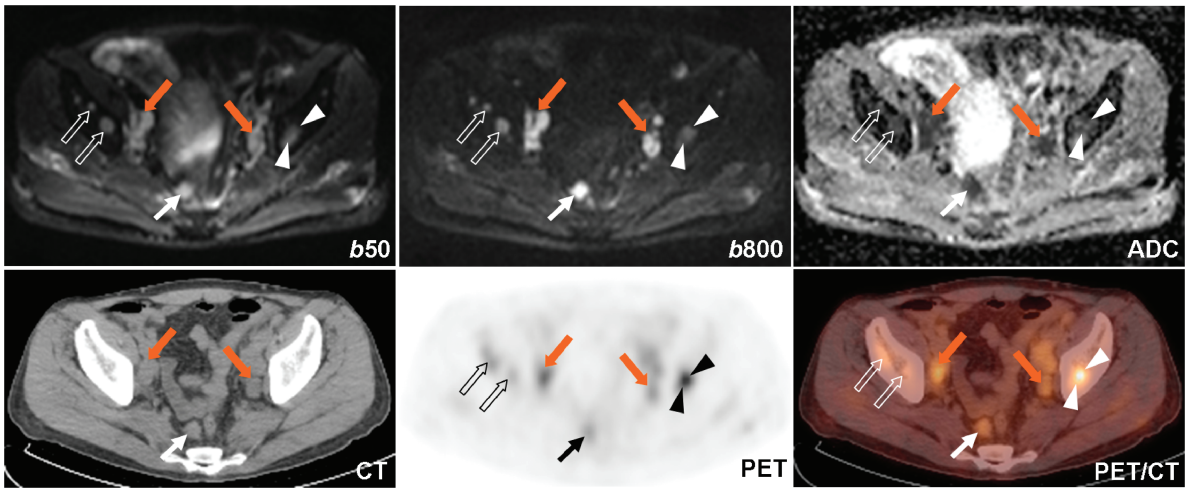

Figure 2 **Diffusion-weighted images with *b* values of 50 and 800 s/mm^2 (*b*50 and *b*800) and their corresponding ADC map (upper row) and integrated FDG-PET/CT images (lower row) in a 57-year-old patient with histologically proven concomitant diffuse large B-cell lymphoma and follicular lymphoma. The lymph node (arrow in white/black) on the sigmoid mesocolon is hyperintense on *b*50 diffusion-weighted images and remains hyperintense on *b*800 diffusion-weighted images; the signal from the intestinal loops and background structures drops significantly. Therefore, this lymph node (mean ADC 0.612×10^{-3} mm^2/s) was easily depicted on diffusion-weighted images along with bilateral iliac nodes (orange arrows), which all show restricted diffusion with signal hypointense to muscle on the ADC map. This sigmoid mesocolon node, however, probably a follicular component, shows relatively low glycolytic activity on PET (maximum SUV 2.9). The left iliac bone lesion (arrowheads) shows more intense FDG uptake, as well as bone lesions at other slice levels (images not shown). One of the bone lesions was proven histologically as a large-cell component. These bone lesions also showed restricted diffusion on the ADC map. Note that FDG uptake by right iliac bone lesions (open arrows) was lower than on the left side, because of their small size. Note also that water diffusion in normal bone marrow is restricted.**

Whole-body DWI in lymphoma

Literature data

Several recent studies have shown the potential of whole-body DWI in lymphoma staging[22–24,27]. Stecco *et al.*[22] included 29 patients for tumor staging with fluorodeoxyglucose (FDG)-PET/computed tomography (CT) as the reference standard. Fifteen of these patients had lymphoma. The histological types of lymphoma for these patients were unknown. They concluded that whole-body DWI using DWIBS can be useful for lymphoma staging because of good delineation of nodal disease[22]. More recently, whole-body magnetic resonance imaging (MRI), including DWI, was evaluated for initial staging in a study including only patients with lymphomas[23]. The results were compared with contrast-enhanced CT. In case of discrepancies, the results were correlated with findings on FDG-PET, bone marrow biopsy or follow-up studies. Overall, initial staging using whole-body MRI (without DWI and with DWI) equals staging using CT in most patients. Whole-body MRI with DWI correctly over staged in 6 (21%) out of 28 patients relative to CT, with a possible advantage of using DWI[23]. However, the authors did not assess the usefulness of whole-body DWI alone for lymphoma staging. In addition, patients with Hodgkin and non-Hodgkin lymphoma (NHL) were included as well as NHL with different histological grades where tissue composition and cellularity may considerably vary. MRI provides good soft tissue contrast, therefore, it should be theoretically advantageous in depicting extranodal disease. However, Kwee *et al.*[24] demonstrated that the ability of whole-body MRI without DWI and with DWI in the detection of bone marrow involvement out of 12 patients with positive bone marrow biopsy (BMB) results was surprisingly low, with patient-based sensitivities of 41.7% and 45.5%, respectively. They speculated that bone marrow involvement in the false-negative patients might have been overlooked in part because of lower spatial resolution applied in the whole-body MR protocol compared with that of dedicated MRI[24]. In 8 other patients, MRI (both without and with DWI) was positive and BMB was negative. BMB may miss focal bone marrow involvement because of limited sampling and further follow-up is needed to provide insight into the rate of correct upstaging by whole-body MRI, including DWI[24].

Our experience

We have conducted a prospective pilot study of 15 patients with histologically proven diffuse large B-cell

lymphoma (DLBCL) using the whole-body respiratory-gated DWI[26]. Among them, 2 patients had concomitant DLBCL and a follicular lymphoma component. FDG-PET is currently a powerful whole-body functional imaging modality and has been shown to be more accurate than contrast-enhanced CT for lymphoma staging in terms of nodal and extranodal involvement[28–30]. In our study, FDG-PET/CT was taken as the reference standard because pathological proof for each lymph node region or organ suspected to have disease involvement is practically and ethically not possible[23,26]. For lymph node involvement, based on the International Working Group (IWG) Cheson's size criteria alone[31], DWI findings matched PET/CT findings in 277 node regions (94%), yielding sensitivity and specificity of 90% and 94%[26]. Among the 82 lymph node regions that were considered positive on both DWI (size criteria alone) and PET/CT, the lymph nodes were visually hypointense to muscle on ADC maps (restricted diffusion) in 73 regions (89%) (Fig. 2). Not all PET-positive lymph nodes had low ADC values. Small lymph nodes adjacent to the lungs and the heart may show falsely high ADC values probably related to heart motion[26], and are not well visualized on DWIBS images with high *b* values[23]. Although it is known that size criteria lack the desired accuracy for characterizing lymph nodes[23,32], our preliminary results show that for pretreatment staging purposes, the ability of DWI for detection of lymph node involvement based on size criteria alone (i.e., node larger than 1 cm on its longest transverse diameter) was comparable with that of FDG-PET/CT. Studies of whole-body MRI using only T2-weighted images (again with size-based analysis) for pediatric lymphoma staging also corroborated this point[33,34]. In our study, when visual ADC analysis was combined with the size measurement, the specificity of DWI increased to 100% but sensitivity decreased to 81%[26] (Fig. 3). Regarding extranodal organ involvement, whole-body DWI agreed with PET/CT in all 20 organs recorded (100%). All organ lesions showed restricted diffusion therefore combining visual ADC analysis would not change the diagnostic performance of DWI for extranodal disease detection[26]. DWI was not able to depict diffuse spleen involvement in one patient because normal spleen already showed restricted diffusion. However, small focal splenic lesions were identified on the respiratory-gated DWI[26]. DWI can be more sensitive than PET in depicting hepatic and renal involvement in some cases[26] (Fig. 4). There was agreement with Ann Arbor stages in 14 (93%) of the 15 patients.

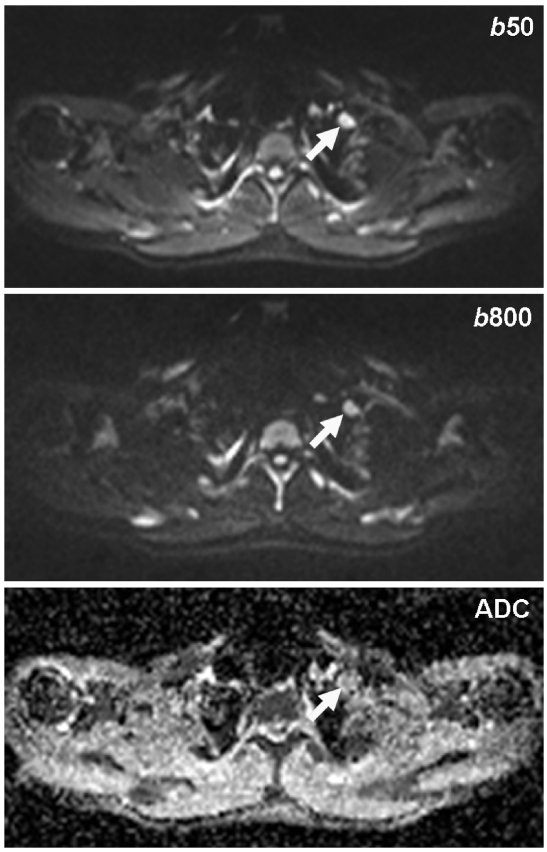

Figure 3 **Diffusion-weighted images with *b* values of 50 and 800 s/mm^2 (*b*50 and *b*800) and their corresponding ADC map in a 24-year-old patient with gastric involvement of diffuse large B-cell lymphoma. In addition to sub-diaphragmatic disease, DWI depicted an additional enlarged lymph node (arrow) on both *b*50 and *b*800 diffusion-weighted images over left lower neck (no abnormal FDG uptake, PET image not shown). DWI upstaged the patient based on size criteria alone. However, this lymph node shows no restricted diffusion (isointense to muscle) on the ADC map. Therefore, with combined ADC analysis, this lymph node can be considered negative, and the patient would have been correctly staged.**

Perspectives

Although size criteria alone may be sufficient for initial lymph node staging, functional information provided by DWI regarding the changes in cellularity, tissue composition and architecture after treatment may be helpful in response assessment. Similar to contrast-enhanced CT, some residual lymph nodes or organ lesions on post-treatment DWI based on size and signal abnormality criteria may not represent viable disease. FDG-PET is more reliable than contrast-enhanced CT in differentiating fibrosis from residual disease and PET information has been incorporated into the revised IWG response criteria[35,36]. A recent study of human DLBCL xenografts showed that DWI can reveal an increase in the mean ADC after as little as 1 week of chemotherapy, preceding changes in the T2 relaxation time[37]. Previously Ballon *et al.*[38] pointed out the potential of DWI in assessing bone marrow signal changes in a patient with leukemia following therapy, indicating a good response. Our

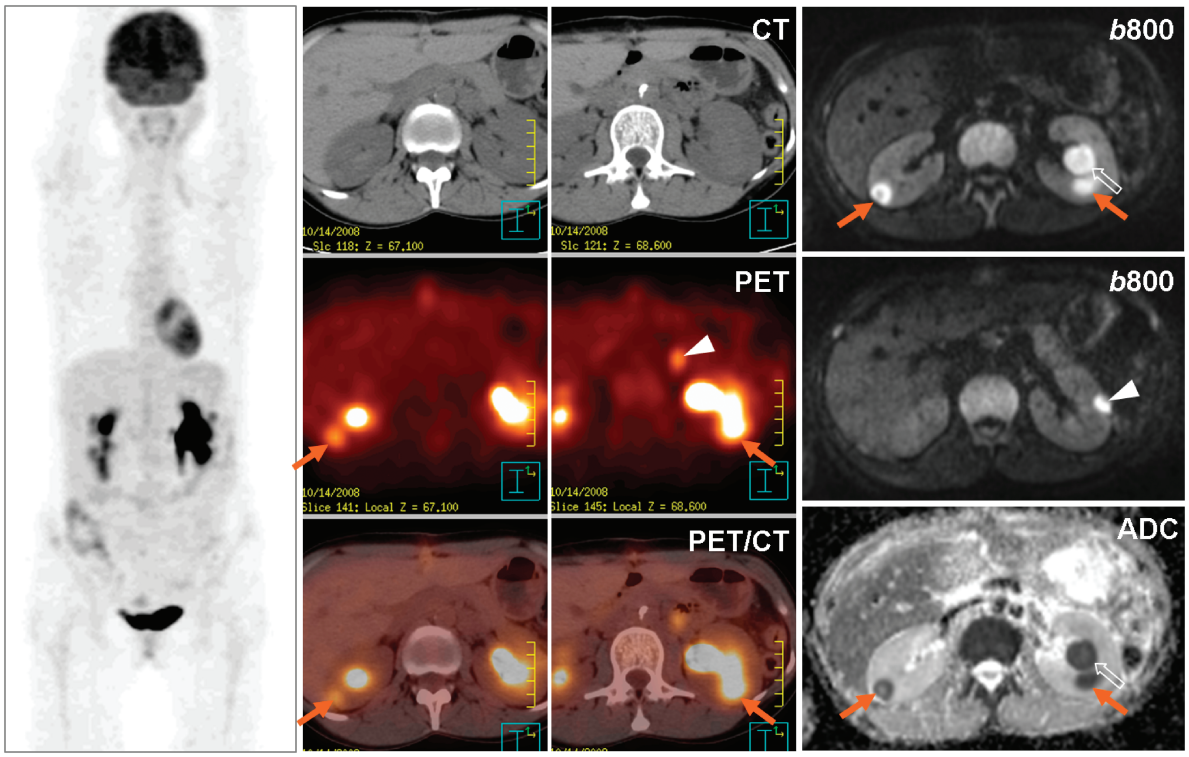

Figure 4 **Whole-body FDG-PET image in maximal intensity projection (left), transverse integrated FDG-PET/CT images (middle two columns) and diffusion-weighted *b*800 images with ADC map (right) in a 42-year-old patient with diffuse large B-cell lymphoma. DWI and PET/CT show focal lesions (arrows) involving both kidneys. However, the mass protruding into the left renal pelvis (open arrow) is obscured by the physiologic FDG excretion on PET; it is clearly depicted on DWI because of excellent lesion-to-normal renal parenchyma contrast. Note that another lesion on the left kidney (arrowhead on *b*800 image) and a lymph node (arrowhead on PET image) were both detected by the other imaging technique on adjacent slices (images not shown).**

preliminary results in patients with DLBCL also showed that post-treatment mean ADC values of residual masses (lymph node regions and organs) on whole-body DWI increased significantly compared with baseline (unpublished data). Thus, combining ADC analysis with size may potentially reduce false-positive findings based on size alone. With good anatomical information provided by *b*50 images and functional and quantitative information provided by the ADC map, whole-body DWI might prove to be valuable for treatment response assessment in patients with lymphoma. There is still room for technical improvement including an EPI sequence with shorter TE and even a non-EPI diffusion-weighted sequence[39,40], which still requires further evaluation for whole-body application.

Conclusion

Contrast-enhanced CT is still the most commonly used imaging modality for staging malignant lymphoma because of its widespread availability and relatively low cost[23,31]. Whole-body DWI does not require contrast medium administration and is superior to CT in depicting extranodal disease involvement. DWI, which reflects tissue structure and cellularity, may be complementary to FDG-PET, which indicates glucose metabolic activity and disease aggressiveness. However, these studies all included relatively small numbers of patients. Future studies with larger patient cohorts and long-term follow-up are necessary to confirm the usefulness of whole-body DWI in the management of patients with lymphoma.

References

[1] Thoeny HC, De Keyzer F. Extracranial applications of diffusion-weighted magnetic resonance imaging. Eur Radiol 2007; 17: 1385–93. doi:10.1007/s00330-006-0547-0. PMid:17206421.

[2] Le Bihan D, Breton E, Lallemand D, Aubin ML, Vignaud J, Laval-Jeantet M. Separation of diffusion and perfusion in intravoxel incoherent motion MR imaging. Radiology 1988; 168: 497–505.

[3] Koh DM, Collins DJ. Diffusion-weighted MRI in the body: applications and challenges in oncology. AJR Am J Roentgenol 2007; 188: 1622–35. doi:10.2214/AJR.06.1403. PMid:17515386.

[4] Abdel Razek AA, Soliman NY, Elkhamary S, Alsharaway MK, Tawfik A. Role of diffusion-weighted MR imaging in cervical lymphadenopathy. Eur Radiol 2006; 16: 1468–77. doi:10.1007/s00330-005-0133-x. PMid:16557366.

[5] Holzapfel K, Duetsch S, Fauser C, Eiber M, Rummeny EJ, Gaa J. Value of diffusion-weighted MR imaging in the differentiation between benign and malignant cervical lymph nodes. Eur J Radiol 2009; 72: 381–7. doi:10.1016/j.ejrad.2008.09.034. PMid: 18995981.

[6] Vandecaveye V, De Keyzer F, Vander Poorten V, *et al.* Head and neck squamous cell carcinoma: value of diffusion-weighted MR imaging for nodal staging. Radiology 2009; 251: 134–46. doi:10.1148/radiol.2511080128. PMid:19251938.

[7] Nasu K, Kuroki Y, Nawano S, *et al.* Hepatic metastases: diffusion-weighted sensitivity-encoding versus SPIO-enhanced MR imaging. Radiology 2006; 239: 122–30. doi:10.1148/radiol.2383041384. PMid:16493012.

[8] Lin G, Ng KK, Chang CJ, *et al.* Myometrial invasion in endometrial cancer: diagnostic accuracy of diffusion-weighted 3.0-T MR imaging–initial experience. Radiology 2009; 250: 784–92. doi:10.1148/radiol.2503080874. PMid:19244045.

[9] Taouli B, Vilgrain V, Dumont E, Daire JL, Fan B, Menu Y. Evaluation of liver diffusion isotropy and characterization of focal hepatic lesions with two single-shot echo-planar MR imaging sequences: prospective study in 66 patients. Radiology 2003; 226: 71–8. doi:10.1148/radiol.2261011904. PMid:12511671.

[10] Moffat BA, Chenevert TL, Lawrence TS, *et al.* Functional diffusion map: a noninvasive MRI biomarker for early stratification of clinical brain tumor response. Proc Natl Acad Sci USA 2005 12; 102: 5524–9.

[11] Dzik-Jurasz A, Domenig C, George M, *et al.* Diffusion MRI for prediction of response of rectal cancer to chemoradiation. Lancet 2002; 360: 307–8. doi:10.1016/S0140-6736(02)09520-X.

[12] Koh DM, Scurr E, Collins D, *et al.* Predicting response of colorectal hepatic metastasis: value of pretreatment apparent diffusion coefficients. AJR Am J Roentgenol 2007; 188: 1001–8. doi:10.2214/AJR.06.0601. PMid:17377036.

[13] Vandecaveye V, Dirix P, De Keyzer F, *et al.* Predictive value of diffusion-weighted magnetic resonance imaging during chemoradiotherapy for head and neck squamous cell carcinoma. Eur Radiol 2010; 20: 1703–14. doi:10.1007/s00330-010-1734-6. PMid:20179939.

[14] Nakayama T, Yoshimitsu K, Irie H, *et al.* Usefulness of the calculated apparent diffusion coefficient value in the differential diagnosis of retroperitoneal masses. J Magn Reson Imaging 2004; 20: 735–42. doi:10.1002/jmri.20149. PMid:15390151.

[15] Sumi M, Ichikawa Y, Nakamura T. Diagnostic ability of apparent diffusion coefficients for lymphomas and carcinomas in the pharynx. Eur Radiol 2007; 17: 2631–7. doi:10.1007/s00330-007-0588-z. PMid:17429643.

[16] Toh CH, Castillo M, Wong AM, *et al.* Primary cerebral lymphoma and glioblastoma multiforme: differences in diffusion characteristics evaluated with diffusion tensor imaging. AJNR Am J Neuroradiol 2008; 29: 471–5. doi:10.3174/ajnr.A0872. PMid:18065516.

[17] Takahara T, Imai Y, Yamashita T, Yasuda S, Nasu S, Van Cauteren M. Diffusion weighted whole body imaging with background body signal suppression (DWIBS): technical improvement using free breathing, STIR and high resolution 3D display. Radiat Med 2004; 22: 275–82.

[18] Kwee TC, Takahara T, Ochiai R, Nievelstein RA, Luijten PR. Diffusion-weighted whole-body imaging with background body signal suppression (DWIBS): features and potential applications in oncology. Eur Radiol 2008; 18: 1937–52. doi:10.1007/s00330-008-0968-z. PMid:18446344.

[19] Koh DM, Takahara T, Imai Y, Collins DJ. Practical aspects of assessing tumors using clinical diffusion-weighted imaging in the body. Magn Reson Med Sci 2007; 6: 211–24. doi:10.2463/mrms.6.211. PMid:18239358.

[20] Komori T, Narabayashi I, Matsumura K, *et al.* 2-[Fluorine-18]-fluoro-2-deoxy-D-glucose positron emission tomography/computed tomography versus whole-body diffusion-weighted MRI for detection of malignant lesions: initial experience. Ann Nucl Med 2007; 21: 209–15. doi:10.1007/s12149-007-0010-6. PMid:17581719.

[21] Ohno Y, Koyama H, Onishi Y, *et al.* Non-small cell lung cancer: whole-body MR examination for M-stage assessment–utility for whole-body diffusion-weighted imaging compared with integrated FDG PET/CT. Radiology 2008; 248: 643–54. doi:10.1148/radiol.2482072039. PMid:18539889.

[22] Stecco A, Romano G, Negru M, *et al.* Whole-body diffusion-weighted magnetic resonance imaging in the staging of oncological patients: comparison with positron emission tomography computed tomography (PET-CT) in a pilot study. Radiol Med 2009; 114: 1–17. doi:10.1007/s11547-008-0348-4. PMid:19082787.

[23] Kwee TC, Quarles van Ufford HM, Beek FJ, *et al.* Whole-body MRI, including diffusion-weighted imaging, for the initial staging of malignant lymphoma: comparison to computed tomography. Invest Radiol 2009; 44: 683–90. doi:10.1097/RLI.0b013e3181afbb36. PMid:19724232.

[24] Kwee TC, Fijnheer R, Ludwig I, *et al.* Whole-body magnetic resonance imaging, including diffusion-weighted imaging, for diagnosing bonerow involvement in malignant lymphoma. Br J Haematol 2010; 149: 628–30. doi:10.1111/j.1365-2141.2010.08093.x. PMid:20128795.

[25] Takahara T, Kwee T, Kibune S, *et al.* Whole-body MRI using a sliding table and repositioning surface coil approach. Eur Radiol 2010; 20: 1366–73. doi:10.1007/s00330-009-1674-1. PMid: 19997846.

[26] Lin C, Luciani A, Itti E, *et al.* Whole-body diffusion-weighted magnetic resonance imaging with apparent diffusion coefficient mapping for staging patients with diffuse large B-cell lymphoma. Eur Radiol 2010; 20: 2027–38. doi:10.1007/s00330-010-1758-y. PMid:20309558.

[27] Li S, Xue HD, Li J, *et al.* Application of whole body diffusion weighted MR imaging for diagnosis and staging of malignant lymphoma. Chin Med Sci J 2008; 23: 138–44. doi:10.1016/S1001-9294(09)60028-6.

[28] Moog F, Bangerter M, Diederichs CG, *et al.* Lymphoma: role of whole-body 2-deoxy-2-[F-18]fluoro-D-glucose (FDG) PET in nodal staging. Radiology 1997; 203: 795–800.

[29] Moog F, Bangerter M, Diederichs CG, *et al.* Extranodal malignant lymphoma: detection with FDG PET versus CT. Radiology 1998; 206: 475–81.

[30] Schaefer NG, Hany TF, Taverna C, *et al.* Non-Hodgkin lymphoma and Hodgkin disease: coregistered FDG PET and CT at staging and restaging–do we need contrast-enhanced CT? Radiology 2004; 232: 823–9. doi:10.1148/radiol.2323030985. PMid:15273335.

[31] Cheson BD, Horning SJ, Coiffier B, *et al.* Report of an international workshop to standardize response criteria for non-Hodgkin's lymphomas. NCI Sponsored International Working Group. J Clin Oncol 1999; 17: 1244.

[32] Torabi M, Aquino SL, Harisinghani MG. Current concepts in lymph node imaging. J Nucl Med 2004; 45: 1509–18.

[33] Kellenberger CJ, Miller SF, Khan M, Gilday DL, Weitzman S, Babyn PS. Initial experience with FSE STIR whole-body MR imaging for staging lymphoma in children. Eur Radiol 2004; 14: 1829–41.

[34] Punwani S, Taylor SA, Bainbridge A, *et al.* Pediatric and adolescent lymphoma: comparison of whole-body STIR half-Fourier RARE MR imaging with an enhanced PET/CT reference for initial staging. Radiology 2010; 255: 182–90. doi:10.1148/radiol.09091105. PMid:20308456.

[35] Juweid ME, Stroobants S, Hoekstra OS, *et al.* Use of positron emission tomography for response assessment of lymphoma: consensus of the Imaging Subcommittee of International Harmonization Project in Lymphoma. J Clin Oncol 2007; 25: 571–8. doi:10.1200/JCO.2006.08.2305. PMid:17242397.

[36] Cheson BD, Pfistner B, Juweid ME, *et al.* Revised response criteria for malignant lymphoma. J Clin Oncol 2007; 25: 579–86. doi:10.1200/JCO.2006.09.2403. PMid:17242396.

[37] Huang MQ, Pickup S, Nelson DS, *et al.* Monitoring response to chemotherapy of non-Hodgkin's lymphoma xenografts by T(2)-weighted and diffusion-weighted MRI. NMR in biomedicine 2008; 21: 1021–9. doi:10.1002/nbm.1261. PMid:18988250.

[38] Ballon D, Watts R, Dyke JP, *et al.* Imaging therapeutic response in human bonerow using rapid whole-body MRI. Magn Reson Med 2004; 52: 1234–8. doi:10.1002/mrm.20291. PMid:15562475.

[39] Juan CJ, Chang HC, Hsueh CJ, *et al.* Salivary glands: echo-planar versus PROPELLER Diffusion-weighted MR imaging for assessment of ADCs. Radiology 2009; 253: 144–52. doi:10.1148/radiol.2531082228. PMid:19789257.

[40] De Foer B, Vercruysse JP, Bernaerts A, *et al.* Middle ear cholesteatoma: non-echo-planar diffusion-weighted MR imaging versus delayed gadolinium-enhanced T1-weighted MR imaging–value in detection. Radiology 2010; 255: 866–72. doi:10.1148/radiol.10091140. PMid:20501723.